Communications in Mathematics and Applications
Vol. 15, No. 3, pp. 1115–1128, 2024
ISSN 0975-8607 (online); 0976-5905 (print)
Published by RGN Publications
DOI: 10.26713/cma.v15i3.2596

http://www.rgnpublications.com

Research Article

A Mathematical Study on SIR Epidemic Model During COVID-19

S. Meenakshi[1], V. Ananthaswamy*[1], J. Anantha Jothi[1] and V. K. Santhi[2]

[1] *Research Centre and PG Department of Mathematics, The Madura College* (*affiliated to Madurai Kamaraj University*), *Madurai, Tamil Nadu, India*
[2] *PG Department of Mathematics, Sri Meenakshi Government Arts College for Women* (*affiliated to Madurai Kamaraj University*), *Madurai, Tamil Nadu, India*
***Corresponding author:** ananthu9777@gmail.com

Received: February 20, 2024 **Accepted:** April 9, 2024

Abstract. In this study, a novel epidemic model for COVID 19 (information propagation model) which explains the dissemination of information is examined. The model is related to the total number of primary communicators, onlookers, secondary communicators, immunizers, as well as quitters at network nodes. The approximate analytical results for the five compartments represented by primary communicators, onlookers, secondary communicators, immunizers as well as quitters are obtained by employing the Homotopy analysis approach. Our approximate analytical expressions are compared with the numerical simulation (MATLAB) and are shown to be a very good fit with all parameter values. The impacts of several parameters including initial transmission rate, propagation rates, exit rate, network average degree along with quit probability are shown in the graphical representation. With the help of this technique, the epidemic models SIR (Susceptible-Infected-Recovered), SVIR (Susceptible-Vaccinated-Infected-Recovered), SEIR (Susceptible-Exposed-Infected-Recovered), SVEIR (Susceptible-Vaccinated-Exposed-Infected-Recovered) of COVID 19, malaria, tuberculosis, and HIV can be readily solved.

Keywords. SIR model, COVID-19, Non-linear initial value problem, Homotopy analysis method, Numerical simulation

Mathematics Subject Classification (2020). 34A05, 34A12, 34E05, 34E10

1. Introduction

A mathematical modelling has developed by Lekone and Finkenstädt [9] as a crucial technique for exploring the dynamics for the transmission of infectious disorders. The most often utilised framework for theory divides the human host population into four categories: susceptible, infected, exposed, infectious, and recovered. Such susceptible-exposed-infectious-recovered (SEIR) representations where typically stated in order a set of differential equations, wherein the rates of flow across compartments are governed by factors particular to the disease's natural history. Daghriri *et al.* [6] highlighted the development of specific epidemiological models, evaluate models critically in regard to the amount and depth of modelling of media platforms, social networking elements, sentiment analysis, and lastly, partially depict the analysis of sentiment employing COVID-19 data collected from Twitter.

Coronavirus disease (COVID-19) is a contagious illness brought on by the SARSCoV-2 virus. As explained by Rangasamy *et al.* [16], epidemic models are often utilised and useful for a variety of applications. Numerous epidemic models are described in the literature, including Susceptible, Infected, Recovered (SIR) as well as its Exposed variants (SEIR), vaccinated (SVIR), SEIR-asymptomatic (SEIAR), SEIAR-vaccinated (SEVIAR), with deceased (SIRD), SVIR-asymptomatic (SAVIR), cross-immunity component (SIRC), as well as with quarantine (SIRQ). In the work of Chowdhury *et al.* [5], a numeric-analytic multistage homotopy-perturbation approach has been used to model the whole time evolution in the prey and predator problem. Additionally, numerical contrasts with the traditional homotopy perturbation technique and the fourth-order Runge-Kutta (RK4) approach were compared numerically and shown. The population is partitioned into four sections in the SEIR model, according to Al-Smadi and Gumah [2], a susceptible compartment, designated S, in which everyone in the population are more susceptible to infectious diseases; and an exposed compartment, designated E; an infected compartment, designated I; and a removed compartment, designated R; and all human beings have been cured of the disease. IMR along with ITR were examined together with a one-step and two-step symmetrization with respect to active as well as passive modes in Bakar and Razali [4] findings for the SEIR model utilising two symmetric Runge-Kutta methods. The Runge-Kutta method along with the fourth order Euler approach was both used by Ashgi *et al.* [3] for solving the SIR Model. The application of SIR and SEIR model are given by Ali and Khan [1], Ebiwareme *et al.* [7], El-Hajji and Albargi [8], Narmatha *et al.* [14], Prodanov [15], Renganathan *et al.* [17], Rustum and Al-Temimi [18], and Zarin *et al.* [19].

The primary goal of this study is to employ the Homotopy analysis technique to obtain approximate analytical outcomes for the SIR model. At present, researchers handle these types of problems while providing implicit solutions, besides our approximate results offers explicit solutions. The approximate analytical findings and numerical simulation are subsequently juxtapose and graphically displayed. In order to distinguish the influence of several parameters like the propagation rates, the exit rate, the network average degree, the quit probability and the initial transmission rate, the graphical representations are illustrated.

2. Mathematical Formulation of the Problem

2.1 Standard SIR Model

According to the SIR model, certain illnesses can be treated and also never infected yet again. Individuals are classified into three phases in the SIR model: susceptible phase S, infected

phase I, and immune phase R. Between them, the infected person will be treated, and soon after getting cured, they will get immunity and will not again be infected, and also is unable to distribute the virus to other people, thus they no longer takes part in the virus's spread. The SIR model's transmission mechanism is as follows: Persons in the susceptible stated S who get close into interaction with people who are in the infection state I may become infected, and those in the infection state I may infect others while also being cured and recovered and then transforming into an immune state R that will never again be infected and disseminate the virus. The flow diagram for SIR model as shown in Figure 1a.

Compared to the SI and SIS models, the SIR-based model is far more accurate. Furthermore, following the dissemination of knowledge via social media during a period of time, people are likely to stop eventually stop disseminating it, which remains more consistent with the SIR model's characteristics. As a result, studying dissemination of information using the SIR model is more applicable.

2.2 Principle Analysis of Information Dissemination Model

The SIR concept of infectious disorders discusses diseases that cannot be infected if the patient is cured. Individuals within the models of SIR are classified into three states as follows: susceptible S, infected I as well as immune R. According to the SIR model, variations in the quantities of all of these three phases are associated with the λ infection rate, which indicates the risk of getting infected whenever the susceptible node comes into contact with the infected phase I node, μ represents the cure rate, which indicates the possibility that the infected condition I node will be subsequently treated. However, in the case of information transmission, users will pick their attitude with regard to information spontaneously based on their individual desires; therefore this will not be static. Because it would be influenced by the surrounding environment and people, the information dissemination model used in this study has been redesigned on the basis of the SIR model as shown in Figure 1b.

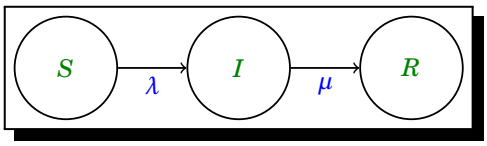

(a) Flow diagram for SIR model

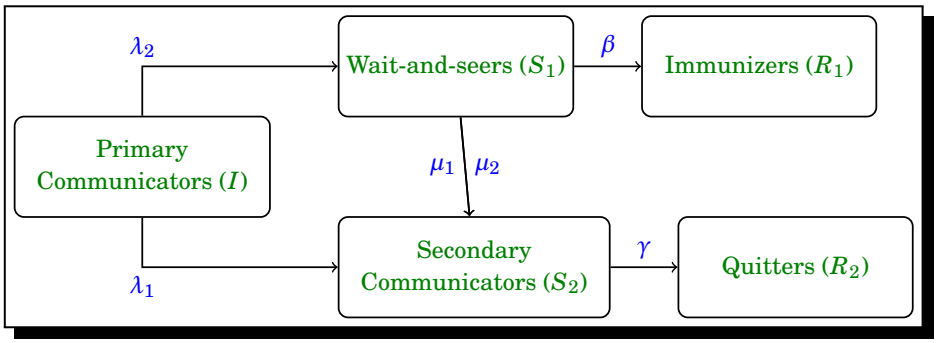

(b) Flow diagram of redesigned SIR model

Figure 1

2.3 An Information Dissemination Model

Here, N represents all of the network's nodes, and $I(t)$, $S_1(t)$, $S_2(t)$, $R_1(t)$, $R_2(t)$ stand for the number of primary communicators, onlookers, secondary communicators, immunizers, together with quitters in the network nodes during time t, and also the $I(t)+S_1(t)+S_2(t)+R_1(t)+R_2(t)=N$ holds. Using an information propagation model, construct the differential equations as indicated below (Zhao and Yu [20]):

$$\frac{dI(t)}{dt} = -\lambda_1 kI(t)S_2(t) - \lambda_2 kI(t)S_2(t), \tag{1}$$

$$\frac{dS_1(t)}{dt} = \lambda_2 kI(t)S_2(t) - (\mu_1+\mu_2)kS_1(t)S_2(t) - [1-(\mu_1+\mu_2)k]\beta S_1(t), \tag{2}$$

$$\frac{dS_2(t)}{dt} = \lambda_1 kI(t)S_2(t) + (\mu_1+\mu_2)kS_1(t)S_2(t) - \gamma S_2(t), \tag{3}$$

$$\frac{dR_1(t)}{dt} = [1-(\mu_1+\mu_2)k]\beta S_1(t), \tag{4}$$

$$\frac{dR_2(t)}{dt} = \gamma S_2(t), \tag{5}$$

where μ_1 and μ_2 stand for the propagation rates, β stands for the exit rate, k means the network average degree, and γ indicates the quit probability. λ_1, λ_2 denotes the initial transmission rate.

With initial conditions

$$\text{At } t=0,\ I(0)=a>0,\ S_1(0)=b>0,\ S_2(0)=d>0,\ R_1(0)=f>0,\ R_2(0)=g>0. \tag{6}$$

3. Approximate Analytical Expression of the Non-Linear Initial Value Problem Using the Homotopy Analysis Method in Information Dissemination Model

The aforementioned first order differential equations are solved utilising the homotopy analysis technique. It is a non-perturbative analytical technique for getting series solutions for equations that are non-linear. The Homotopy analysis technique is an effective analytical technique for non-linear problems, has been developed by Liao [10–13]. With HAM, we may control and regulate the convergence of a solution by utilising the so-called convergence-control parameter, which sets it apart from other perturbative and also non-perturbative analytical methods. Based on this, HAM has become the most effective method for locating analytical results for the function that is unknown along with its derivatives. Previous applications for HAM have mostly concentrated upon non-linear differential equations whereas nonlinearity corresponds to a polynomial, as demonstrated by Liao's work [10, 12, 13].

The approximate analytical expressions of equations (1)-(5) as follows:

$$I(t) = a + \left(\frac{hA_1+hA_2}{A_3}\right)[1-e^{-A_3t}], \tag{7}$$

$$S_1(t) = be^{-B_1t} + \left(\frac{hB_3e^{-B_1t}}{B_1+B_2}\right)[e^{(B_1+B_2)t}-1] + \left(\frac{hB_4e^{-B_1t}}{B_2}\right)[e^{B_2t}-1], \tag{8}$$

$$S_2(t) = de^{-D_1t} + hD_2te^{-D_1t} + \left(\frac{hD_3}{D_4}\right)e^{-D_1t}[e^{D_4t}-1], \tag{9}$$

where

$$R_1(t) = f + b(e^{-F_1 t} - 1), \tag{10}$$

$$R_2(t) = g + h(e^{B_2 t} - 1), \tag{11}$$

where

$$\left.\begin{aligned} &A_1 = \lambda_1 kad,\ A_2 = \lambda_2 kad,\ B_1 = [1-(\mu_1+\mu_2)k]\beta,\ B_2 = -\gamma, B_3 = -\lambda_2 kad,\\ &B_4 = (\mu_1+\mu_2)kbd,\ D_1 = \gamma,\ D_2 = -\lambda_1 kad,\ D_3 = -(\mu_1+\mu_2)kbd,\\ &D_4 = -[1-(\mu_1+\mu_2)k]\beta,\ F_1 = [1-(\mu_1+\mu_2)k]\beta. \end{aligned}\right\} \tag{12}$$

4. Numerical Simulation

Moreover, the function maingraph through MATLAB programme is utilized to solve numerically the given non-linear differential equations (1) to (6). A comparison is made between the numerical simulation and the approximate analytical results. Appendix B has the MATLAB programme. Figure 1c to Figure 6 shows the numerical simulation carried out using MATLAB , together with the approximate analytical expressions that were obtained. An excellent fit is observed.

5. Results and Discussions

Appendix A provides an explanation of the solutions that have been obtained through the use of HAM. Figure 1c depicts the influence of five compartments such as prime communicators $I(t)$, onlookers $S_1(t)$, secondary communicators $S_2(t)$, immunizers $R_1(t)$, and quitters $R_2(t)$ by fixing the appropriate values of all variable.

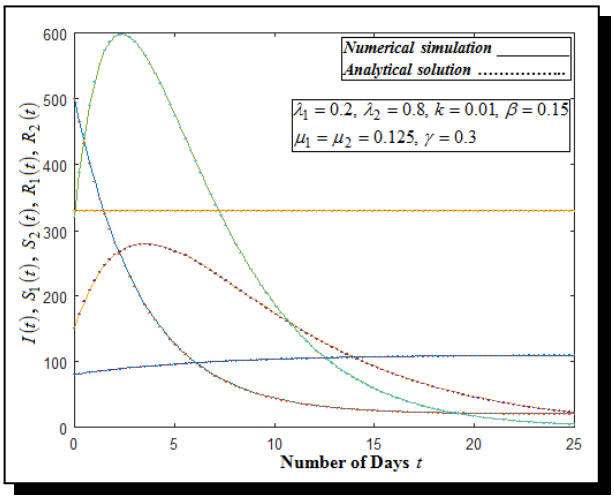

(c) Influence of all parameters in primary communicators $I(t)$, onlookers $S_1(t)$, secondary communicators $S_2(t)$, immunizers $R_1(t)$, quitters $R_2(t)$

Figure 1

For Primary communicators: Figure 2 shows that the primary communicators $I(t)$ with number of days t by utilizing equation (7). Figures 2a and 2c shows that primary communicators $I(t)$ get drops by raising the amounts of transmission rate λ_1 and network average degree k. As seen in Figure 2b, it depicts that primary communicators $I(t)$ get raises by raising the amounts of quit probability γ.

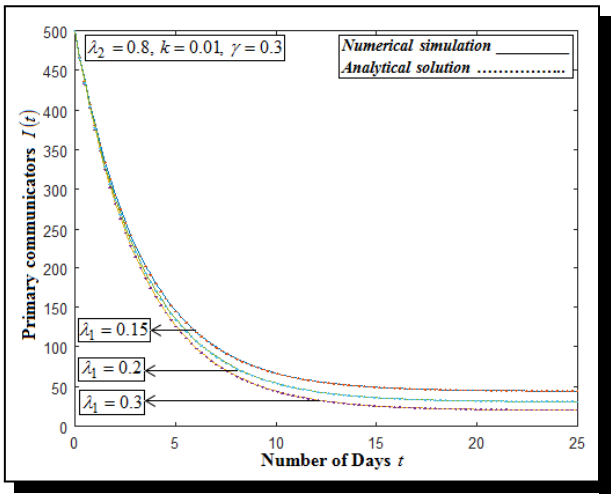

(a) Effects of transmission rate λ_1 in primary communicators $I(t)$

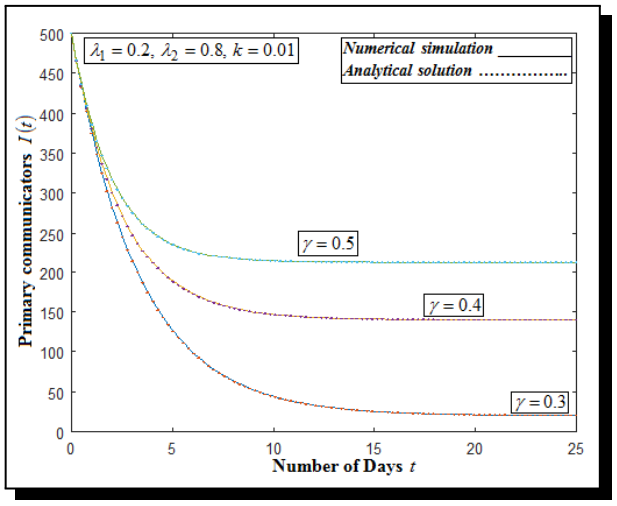

(b) Impact of quit probability γ for primary communicators $I(t)$

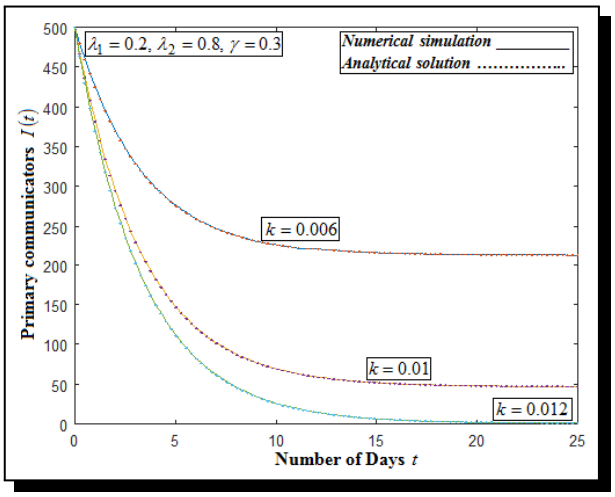

(c) Variation of network average degree k on primary communicators $I(t)$

Figure 2

For Onlookers: Figure 3 displays that the onlookers$S_1(t)$ against the number of days t by employing equation (8). Figures 3a-3c demonstrate how raising the propagation rates μ_1, μ_2, exit rate $\beta$and quit probability γ reduces the number of onlookers $S_1(t)$. As the network average degree k rises, so does the onlookers $S_1(t)$, as illustrated in Figure 3d.

For Secondary Communicators: Figure 4 exhibits that the secondary communicators $S_2(t)$ versus number of days t by using equation (9). Figures 4a and 4b demonstrate when increasing the amounts of quit probability γ and exit rate β results a drop in the secondary communicators $S_2(t)$. Figures 4c and 4d depicts that when raising the values of propagation μ_1, μ_2 and transmission rates λ_1 results in the secondary communicators to grows.

For Immunizers: Figure 5 demonstrates that the immunizers $R_1(t)$ with number of days t by utilizing equation (10). Figures 5a and 5b indicates that immunizers increase when propagation rates μ_1, μ_2 and exit rate β rise.

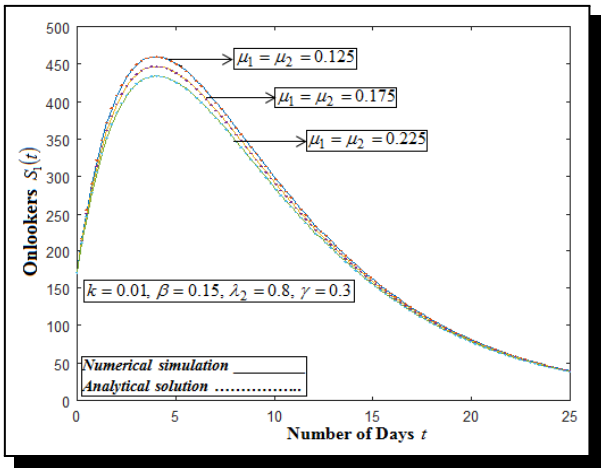

(a) Influence of propagation rates μ_1, μ_2, for onlookers $S_1(t)$

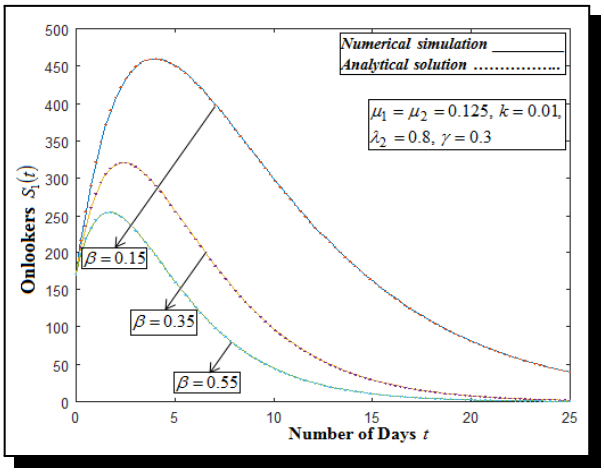

(b) Effect of exit rate β for onlookers $S_1(t)$

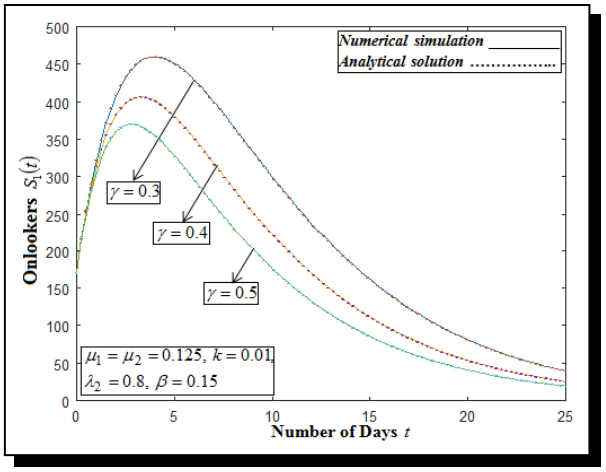

(c) Impact of quit probability γ in onlookers $S_1(t)$

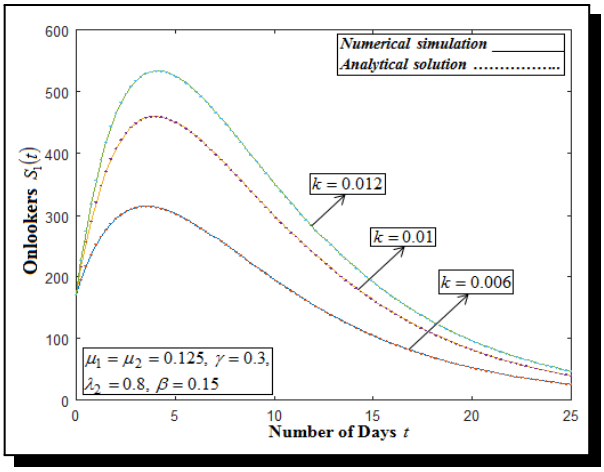

(d) Variation of network average degree k for onlookers $S_1(t)$

Figure 3

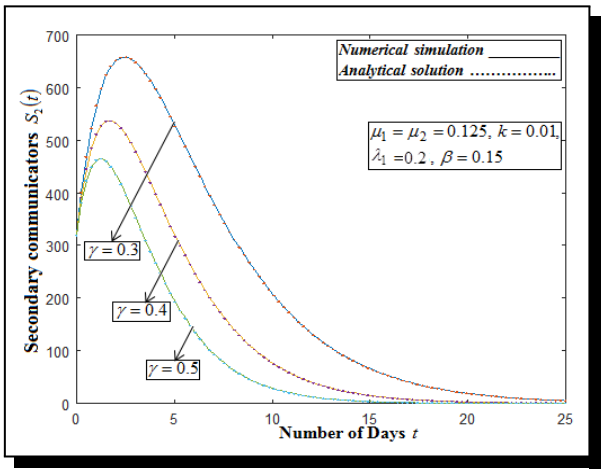

(a) Influence of quit probability γ for secondary communicators $S_2(t)$

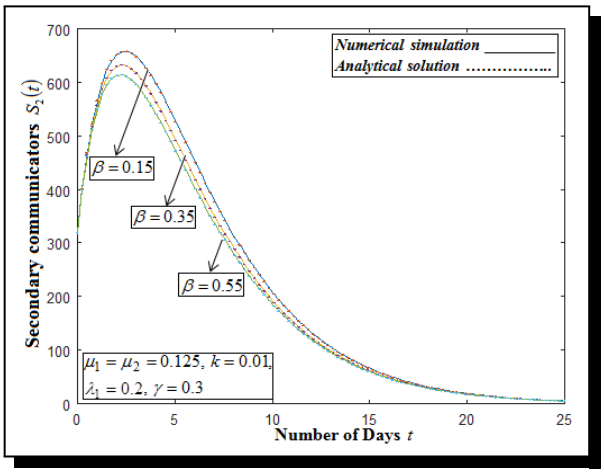

(b) Effect of exit rate β for communicators $S_2(t)$

(Figure *Contd.*)

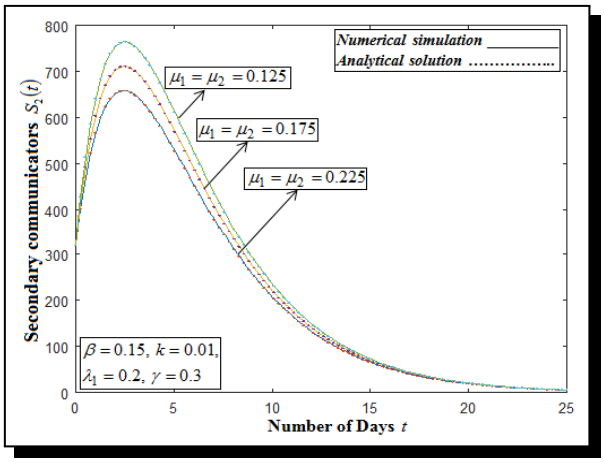

(c) Impact of propagation rates μ_1, μ_2, for secondary communicators $S_2(t)$

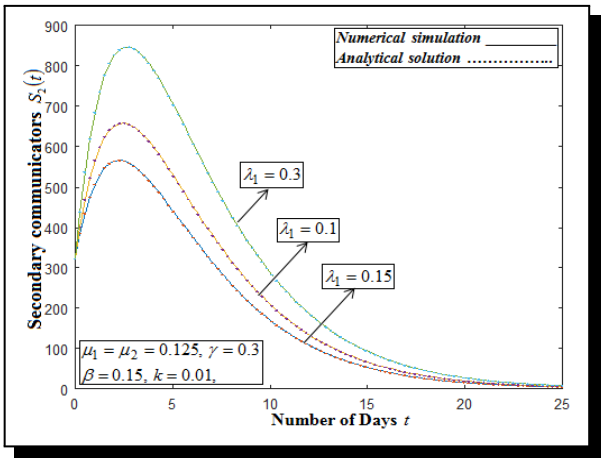

(d) Variation for transmission rate λ_1 in secondary communicators $S_2(t)$

Figure 4

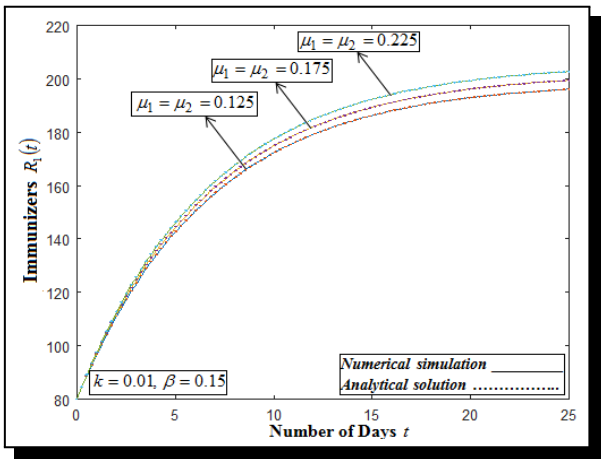

(a) Influence of propagation rates μ_1, μ_2, on immunizers $R_1(t)$

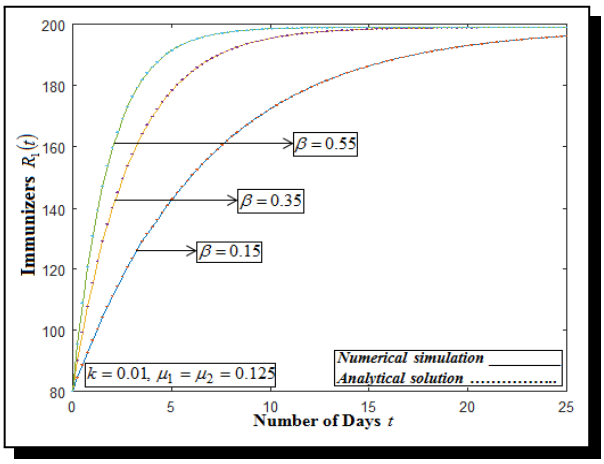

(b) Effect of exit rate β on immunizers $R_1(t)$

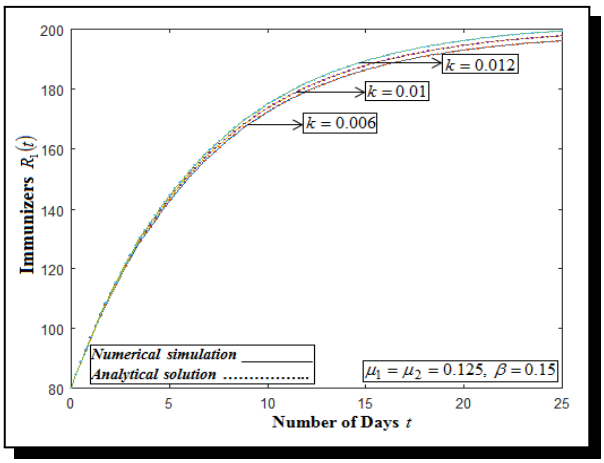

(c) Impact for network average degree k in immunizers $R_1(t)$

Figure 5

For Quitters: Figure 6 displays that the quitters $R_2(t)$ with number of days t by using equation (11). Figure 6 illustrates that when quit probability γ grows, so does the quitters $R_2(t)$.

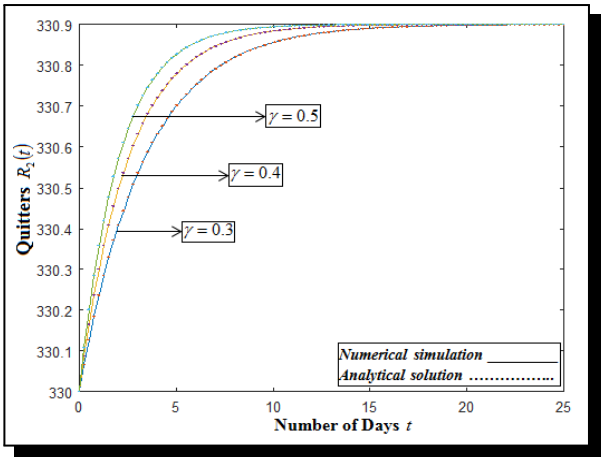

Figure 6. Variation of quit probability γ on quitters $R_2(t)$

6. Conclusion

The approximate analytical solutions for the immunizers, quitters, onlookers, secondary communicators, and primary communicators in the network nodes at time t were presented in this study. The approximate analytical solutions were obtained with the help of the Homotopy analysis technique. The outcomes were matched with the numerical results exactly for small values of the parameters. By changing the values of the initial transmission rate, propagation rate, exit rate, network average degree, and quit probability, the graphs were able to demonstrate the effects of various parameters. The approximate analytical outcomes enable researchers to know more about the model and determine how various factors affect the populations.

The following are observed in the above results:

- As the quit probability γ grows, so does the number of immunizers $R_1(t)$ as well as the number of quitters $R_2(t)$.
- The number of secondary communicators $S_2(t)$ rises as the original transmission rates λ_1 grows.
- As the exit rate β rises, so does the number of immunizers $R_1(t)$.

Appendix A. Approximate Analytical Solution of the Equations (1)-(6) By Employing the Homotopy Analysis Technique

In this appendix, approximate analytical solution of equations (1)-(5) by using the initial condition (6) has been derived briefly.

In order to construct the homotopy for equations (1)-(5), we do the following:

$$(1-p)\left[\frac{dI}{dt}\right] = hp\left[\frac{dI}{dt} + \lambda_1 kIS_2 + \lambda_2 kIS_2\right], \tag{A.1}$$

$$(1-p)\left[\frac{dS_1}{dt} + [1-(\mu_1+\mu_2)k]\beta S_1\right] = hp\left[\frac{dS_1}{dt} - \lambda_2 kIS_2 + (\mu_1+\mu_2)kS_1S_2 + [1-(\mu_1+\mu_2)k]\beta S_1\right], \tag{A.2}$$

$$(1-p)\left[\frac{dS_2}{dt}+\gamma S_2\right]=hp\left[\frac{dS_2}{dt}-\lambda_1 kIS_2-(\mu_1+\mu_2)kS_1S_2+\gamma S_2\right], \tag{A.3}$$

$$(1-p)\left[\frac{dR_1}{dt}\right]=hp\left[\frac{dR_1}{dt}-[1-(\mu_1+\mu_2)k]\beta S_1\right], \tag{A.4}$$

$$(1-p)\left[\frac{dR_2}{dt}\right]=hp\left[\frac{dR_2}{dt}-\gamma S_2\right]. \tag{A.5}$$

Let the initial approximation solutions of the equations (A.1)-(A.5) as follows:

$$I=I_0+pI_1+p^2I_2+\ldots, \tag{A.6}$$

$$S_1=S_{1_0}+pS_{1_1}+p^2S_{1_2}+\ldots, \tag{A.7}$$

$$S_2=S_{2_0}+pS_{2_1}+p^2S_{2_2}+\ldots, \tag{A.8}$$

$$R_1=R_{1_0}+pR_{1_1}+p^2R_{1_2}+\ldots, \tag{A.9}$$

$$R_2=R_{2_0}+pR_{2_1}+p^2R_{2_2}+\ldots. \tag{A.10}$$

Consequently, the initial conditions are

$$\left.\begin{aligned} &I_0(0)=a>0,\ S_{1_0}(0)=b>0,\ S_{2_0}(0)=d>0,\ R_{1_0}(0)=f>0,\ R_{2_0}(0)=g>0,\\ &I_i(0)=0,\ S_{1_i}(0)=0,\ S_{2_i}(0)=0,\ R_{1_i}(0)=0,\ R_{2_i}(0)=0,\ i=1,2,3\ldots. \end{aligned}\right\}. \tag{A.11}$$

Equating the coefficients of p^0 after substituting equations (A.6)-(A.10) in equations (A.1)-(A.5) yields the following:

$$\frac{dI_0}{dt}=0, \tag{A.12}$$

$$\frac{dS_{1_0}}{dt}+[1-(\mu_1+\mu_2)k]\beta S_{1_0}=0, \tag{A.13}$$

$$\frac{dS2_0}{dt}+\gamma S_{2_0}=0, \tag{A.14}$$

$$\frac{dR_{1_0}}{dt}=0, \tag{A.15}$$

$$\frac{dR_{2_0}}{dt}=0. \tag{A.16}$$

Now, by solving the equations (A.12)-(A.16) utilising the initial conditions from equation (A.11), we obtain

$$I_0=a, \tag{A.17}$$

$$S_{1_0}=be^{-[1-(\mu_1+\mu_2)k]\beta t}, \tag{A.18}$$

$$S_{2_0}=de^{-\gamma t}, \tag{A.19}$$

$$R_{1_0}=f, \tag{A.20}$$

$$R_{2_0}=g. \tag{A.21}$$

After equating p^1 coefficients, we have

$$\frac{dI_1}{dt}-\frac{dI_0}{dt}=h\left[\frac{dI_0}{dt}+\lambda_1 kI_0S_{2_0}+\lambda_2 kI_0S_{2_0}\right], \tag{A.22}$$

$$\frac{dS_{1_1}}{dt}+[1-(\mu_1+\mu_2)k]\beta S_{1_1}-\left(\frac{dI_0}{dt}+[1-(\mu_1+\mu_2)k]\beta S_{1_1}\right)$$
$$=h\left[\frac{dI_0}{dt}+[1-(\mu_1+\mu_2)k]\beta S_{1_1}-\lambda_2 kI_0S_{2_0}+(\mu_1+\mu_2)kS_{1_0}S_{2_0}\right], \tag{A.23}$$

$$\frac{dS_{2_1}}{dt}+\gamma S_{2_1}-\left(\frac{dS_{2_0}}{dt}+\gamma S_{2_0}\right)=h\left[\frac{dS_{2_0}}{dt}+\gamma S_{2_0}-\lambda_1 kI_0S_{2_0}-(\mu_1+\mu_2)kS_{1_0}S_{2_0}\right], \tag{A.24}$$

$$\frac{dR_{1_1}}{dt}-\frac{dR_{1_0}}{dt}=h\left[\frac{dR_{1_0}}{dt}-[1-(\mu_1+\mu_2)k]\beta S_{1_0}\right], \tag{A.25}$$

$$\frac{dR_{2_1}}{dt}-\frac{dR_{2_0}}{dt}=h\left[\frac{dR_{2_0}}{dt}-\gamma S_{2_0}\right]. \tag{A.26}$$

Equations (A.22)-(A.26) can be solved by employing the initial conditions found in equation (A.11), we attain

$$I_1=\left(\frac{hkad(\lambda_1+\lambda_2)}{\gamma}\right)[1-e^{-\gamma t}], \tag{A.27}$$

$$S_{1_1}=\left(\frac{h(-\lambda_2 kad)e^{-[1-(\mu_1+\mu_2)k]\beta t}}{[1-(\mu_1+\mu_2)k]\beta-\gamma}\right)[e^{([1-(\mu_1+\mu_2)k]\beta-\gamma)t}-1]$$
$$+\left(\frac{h(\mu_1+\mu_2)kbde^{-[1-(\mu_1+\mu_2)k]\beta t}}{-\gamma}\right)[e^{-\gamma t}-1], \tag{A.28}$$

$$S_{2_1}=h(-\lambda_1 kad)te^{-\gamma t}+\left(\frac{h(-(\mu_1+\mu_2)kbd)}{-[1-(\mu_1+\mu_2)k]\beta}\right)e^{-\gamma t}[e^{-[1-(\mu_1+\mu_2)k]\beta t}-1], \tag{A.29}$$

$$R_{1_1}=hb(e^{-[1-(\mu_1+\mu_2)k]\beta t}-1), \tag{A.30}$$

$$R_{2_1}=h(e^{-\gamma t}-1). \tag{A.31}$$

Equations (A.17) and (A.27) are added, we yield

$$I=I_0+I_1=a+\left(\frac{hkad(\lambda_1+\lambda_2)}{\gamma}\right)[1-e^{-\gamma t}]. \tag{A.32}$$

The result of adding equations (A.18) and (A.28) is

$$S_1=S_{1_0}+S_{1_1}=be^{-[1-(\mu_1+\mu_2)k]\beta t}$$
$$+\left(\frac{h(-\lambda_2 kad)e^{-[1-(\mu_1+\mu_2)k]\beta t}}{([1-(\mu_1+\mu_2)k]\beta-\gamma)}\right)[e^{([1-(\mu_1+\mu_2)k]\beta-\gamma)t}-1]$$
$$+\left(\frac{h(\mu_1+\mu_2)kbde^{-[1-(\mu_1+\mu_2)k]\beta t}}{-\gamma}\right)[e^{-\gamma t}-1]. \tag{A.33}$$

Equations (A.19) and (A.29) are added to yield

$$S_2=S_{2_0}+S_{2_1}=de^{-\gamma t}+h(-\lambda_1 kad)te^{-\gamma t}$$
$$+\left(\frac{h(-(\mu_1+\mu_2)kbd)}{-[1-(\mu_1+\mu_2)k]\beta}\right)e^{-\gamma t}[e^{-[1-(\mu_1+\mu_2)k]\beta t}-1]. \tag{A.34}$$

Equations (A.20) and (A.30) are added, getting:

$$R_1=R_{1_0}+R_{1_1}=f+hb(e^{-[1-(\mu_1+\mu_2)k]\beta t}-1). \tag{A.35}$$

Equations (A.21) and (A.31) added together obtain

$$R_2=R_{2_0}+R_{2_1}=g+h(e^{-\gamma t}-1). \tag{A.36}$$

Hence the approximate analytical results for five compartments were attained in equations (A.32)-(A.36).

Appendix B. MATLAB Programming for Equations (1)-(6)

```
function maingraph
options=odeset('RelTol',1e-6,'Stats','on');
\%initial conditions
Xo=[500,170,320, 80,5];
tspan=[0 30];ss
tic
[t,X]=ode45(@TestFunction,tspan,Xo,options);
toc
figure
hold on
plot(t,X(:,1),'-')
plot(t,X(:,2),'-')
plot(t,X(:,3),'-')
plot(t,X(:,4),'-')
plot(t,X(:,5),'-')
legend('Susceptible','Exposed','Infected','Recovered','I')
ylabel('Population')
xlabel('Time')
return
function[dx_dt]=TestFunction(~,x)
k=0.01;lambda1=0.2;meu1=0.125;meu2=0.125;lambda2=0.8;beta=0.15;gamma=0.3;
dx_dt(1)=-lambda1*k*x(1)*x(3)-lambda2*k*x(1)*x(3);
dx_dt(2)=lambda2*k*x(1)*x(3)-(meu1+meu2)*k*x(2)*x(3)-(1-(meu1+meu2)*k)*beta*x(2);
dx_dt(3)=lambda1*k*x(1)*x(3)+(meu1+meu2)*k*x(2)*x(3)-gamma*x(3);
dx_dt(4)=(1-(meu1+meu2)*k)*beta*x(2);
dx_dt(5)=gamma*x(3);
dx_dt = dx_dt';
return
```

Appendix C. Nomenclature

Symbols	Meaning
N	Total number of nodes
I	Number of primary communicators
S_1	Number of onlookers
S_2	Number of secondary communicators
R_1	Number of immunizers
R_2	Number of quitters
t	Time
λ_1, λ_2	Initial transmission rate
μ_1, μ_2	Propagation rates
β	Exit rate
k	Network average degree
γ	Quit probability

Competing Interests

The authors declare that they have no competing interests.

Authors' Contributions

All the authors contributed significantly in writing this article. The authors read and approved the final manuscript.

References

[1] I. Ali and S. U. Khan, Dynamics and simulations of stochastic COVID-19 epidemic model using Legendre spectral collocation method, *AIMS Mathematics* **8**(2) (2023), 4220 – 4236, DOI: 10.3934/math.2023210.

[2] M. H. AL-Smadi and G. N. Gumah, On the homotopy analysis method for fractional SEIR epidemic model, *Research Journal of Applied Sciences, Engineering and Technology* **7**(18) (2014), 3809 – 3820, DOI: 10.19026/rjaset.7.738.

[3] R. Ashgi, M. A. A. Pratama and S. Purwani, Comparison of numerical simulation of epidemiological model between Euler method with 4th order RungeKutta method, *International Journal of Global Operations Research* **2**(1) (2021), 37 – 44.

[4] S. S. Bakar and N. Razali, Solving SEIR model using symmetrized Runge Kutta methods, in: *Proceedings of the International Conference on Mathematical Sciences and Statistics 2022* (*ICMSS 2022*), N. Wahi, M. A. M. Safari, R. Hasni, F. A. Razak, I. Gafurjan and A. Fitrianto (editors), Advances in Computer Science Research series, pp. 411 – 425, Atlantis Press, DOI: 10.2991/978-94-6463-014-5_36.

[5] M. S. H. Chowdhury, I. Hashim and R. Roslan, Simulation of the predator-prey problem by the homotopy-perturbation method revised, *Topological Methods in Nonlinear Analysis* **31**(2) (2008), 263 – 270, URL: https://projecteuclid.org/journals/topological-methods-in-nonlinear-analysis/volume-31/issue-2/Simulation-of-the-predator-prey-problem-by-thehomotopy-perturbation-method/tmna/1463150270.full.

[6] T. Daghriri, M. Proctor and S. Matthews, Evolution of select epidemiological modeling and the rise of population sentiment analysis: A literature review and COVID-19 sentiment illustration, *International Journal of Environmental Research and Public Health* **19**(6) (2022), 3230, DOI: 10.3390/ijerph19063230.

[7] L. Ebiwareme, R. E. Akpodee and R. I. Ndu, An application of LADM-Padé approximation for the analytical solution of the SIR infectious Disease model, *International Journal of Innovation Engineering and Science Research* **6**(2) (2022), 16 – 30, URL: https://www.ijiesr.com/liebrary/e35/932424858A.pdf.

[8] M. El Hajji and A. H. Albargi, A mathematical investigation of an "SVEIR" epidemic model for the measles transmission, *Mathematical Biosciences and Engineering* **19**(3) (2022), 2853 – 2875, DOI: 10.3934/mbe.2022131.

[9] P. E. Lekone and B. F. Finkenstädt, Statistical inference in a stochastic epidemic SEIR model with control intervention: Ebola as a case study, *Biometrics* **62**(4) (2006), 1170 – 1177, DOI: 10.1111/j.1541-0420.2006.00609.x.

[10] S.-J. Liao, A kind of approximate solution technique which does not depend upon small parameters — II. An application in fluid mechanics, *International Journal of Non-Linear Mechanics* **32**(5) (1997), 815 – 822, DOI: 10.1016/S0020-7462(96)00101-1.

[11] S.-J. Liao, A uniformly valid analytic solution of two-dimensional viscous flow over a semi-infinite flat plate, *Journal of Fluid Mechanics* **385** (1999), 101 – 128, DOI: doi:10.1017/s0022112099004292.

[12] S.-J. Liao, An approximate solution technique not depending on small parameters: A special example, *International Journal of Non-Linear Mechanics* **30**(3) (1995), 371 – 380, DOI: 10.1016/0020-7462(94)00054-e.

[13] S.-J. Liao, An explicit, totally analytic approximate solution for Blasius' viscous flow problems, *International Journal of Non-Linear Mechanics* **34**(4) (1999), 759 – 778, DOI: 10.1016/s0020-7462(98)00056-0.

[14] S. Narmatha, V. Ananthaswamy, S. Sivasundaram and M. Subha, Semi analytical solution to a SIR model using new approach to homotopy perturbation method, *Mathematics in Engineering, Science and Aerospace* **13**(4) (2022), p. 1053, URL: https://nonlinearstudies.com/index.php/mesa/article/view/3018.

[15] D. Prodanov, Chapter 10 - Analytical solutions and parameter estimation of the SIR epidemic model, *Mathematical Analysis of Infectious Diseases*, (2022), 163 – 189, DOI: 10.1016/B978-0-32-390504-6.00015-2.

[16] M. Rangasamy, C. Chesneau, C. Martin-Barreiro and V. Leiva, On a novel dynamics of SEIR epidemic models with a potential application to COVID-19, *Symmetry* **14**(7) (2022), 1436, DOI: 10.3390/sym14071436.

[17] K. Renganathan, V. Ananthaswamy and S. Narmatha, Mathematical analysis of prey predator system with immigrant prey using a new approach to Homotopy perturbation method, *Materials Today: Proceedings* **37**(2) (2021), 1183 – 1189, DOI: 10.1016/j.matpr.2020.06.354.

[18] N. S. Rustum and S. A. S. Al-Temimi, Estimation of the epidemiological model with a system of differential equations (SIRD) using the Runge-Kutta method in Iraq, *International Journal of Nonlinear Analysis and Applications* **13**(2) (2022), 2807 – 2814, DOI: 10.22075/IJNAA.2022.6509.

[19] R. Zarin, Siraj-ul-Islam, N. Haider and Naeem-ul-Islam, Numerical solution of COVID-19 pandemic model via finite difference and meshless techniques, *Engineering Analysis with Boundary Elements* **147** (2023), 76 – 89, DOI: 10.1016/j.enganabound.2022.11.026.

[20] B. Zhao and T. Yu, Biostatistical analysis on the "Information Cocoon Room" during the COVID-19 epidemic, *HSOA Journal of Advances in Microbiology Research* **6**(2023), 019, DOI: 10.24966/AMR-694X/100019.